Catal Lett (2012) 142:445–451
DOI 10.1007/s10562-012-0790-8

Effective Utilization of the Catalytically Active Phase: NH_3 Oxidation Over Unsupported and Supported Co_3O_4

W.-K. Fung · M. Claeys · E. van Steen

Received: 21 October 2011 / Accepted: 24 February 2012 / Published online: 13 March 2012

Abstract The performance of pellets of unsupported and silica-supported Co_3O_4 in the ammonia oxidation was investigated as a function of the particle size to investigate the utilization of the catalytically active phase in these materials. The obtained activity in terms of ammonia conversion over the silica-supported Co_3O_4 is higher compared to the conversion over the unsupported Co_3O_4, despite a lower cobalt oxide loading and more severe diffusional limitations. The effectiveness factor for the silica-supported catalyst is slightly lower than the effectiveness factor for the unsupported catalyst in the form of pellets of similar size. However, the effective utilization of cobalt within the catalyst is higher for the silica-supported catalyst, mainly due to the higher dispersion of the catalytically active phase.

Keywords Ammonia oxidation · Mass transfer · Co_3O_4 · Supported catalyst · Unsupported catalyst · Effectiveness factor

1 Introduction

Ammonia oxidation yielding NO/NO_2 forms the core of the nitric acid production plant. This process typically uses platinum–rhodium gauze as a catalyst for the ammonia oxidation being active (conversions in excess of 90 % can easily be achieved at temperatures between 810 and 940 °C and pressures between 1 and 10 bar) and highly selective [1]. Higher reaction pressures are used for the production of concentrated nitric acid, whereas low pressures can be used for the production of dilute nitric acid. Operation at high pressure comes at the cost of lower NO yield and shorter catalyst life time [2]. In particular, the platinum loss during the process due to platinum volatilization contributes to the high operating costs [1].

Platinum loss can only be minimized but not eliminated, thus a variety of transition metal oxides for the oxidation of ammonia yielding nitrogen oxides have been studied [2–5]. Among simple transition metal oxides, Co_3O_4 was shown to be the most active in the ammonia oxidation exhibiting high activity and high selectivity towards NO [2–5] and is utilized in some nitric acid plants [6] (and lately interest in mixed metal oxides as catalyst for the ammonia oxidation has grown [7–10]). Co_3O_4 seems to have the added advantage of lower yield of the undesirable greenhouse gas N_2O and longer catalyst life time [6].

The unsupported Co_3O_4 catalysts for the ammonia oxidation typically contain large crystallites of the catalytically active phase. For instance, Schmidt-Szalowski et al. [5] demonstrated the usefulness of Co_3O_4 as a catalyst for the ammonia oxidation using Co_3O_4 with an average crystallite size of 80 nm. The utilisation of the catalytically active material can be improved by using materials with a high surface to volume ratio, i.e. small crystallites. However, small crystallites may be more prone to sintering: a process, which can be mitigated by physically separating the crystallites and dispersing them on a support. This is the typical role of a carrier, in addition to controlling the porous structure and enhancing the mechanical strength [11]. Supported catalysts may have an additional benefit for fast reactions operating under internal mass transfer limitations. The distribution of the catalytically active phase over a carrier results in a lower rate per unit volume of

W.-K. Fung · M. Claeys · E. van Steen (✉)
Department of Chemical Engineering, Centre for Catalysis Research, University of Cape Town, Cape Town, Private Bag X3, Rondebosch 7701, South Africa
e-mail: eric.vansteen@uct.ac.za

catalyst, which is the determining factor for the decrease in the concentration of the reactants within a catalyst particle of a given size. In this paper, we will give an example on how supporting the catalytically active material can improve the effective utilisation of the catalytically active material in the ammonia oxidation yielding NO_x.

2 Experimental

The unsupported Co_3O_4, a catalyst commercially used for the ammonia oxidation, was in the form of pellets ($d = 3$ mm; $h = 3$ mm) with a pellet density of 3.54 g/cm^3 and a pore volume of 0.12 cm^3/g resulting in a porosity of 0.42. The pellets contain mainly macro-pores with an average pore diameter of ca. 1.3 μm. The pellet contains an irregular distribution of Co_3O_4 crystallites ranging from 200 nm to 5 μm, with the smaller crystallites seemingly attached to the large crystallites. The pellets were crushed to a size between 75 and 1,000 μm to investigate the effect of the particle size.

Pellets of a silica-supported Co_3O_4 catalyst with a uniform distribution of Co_3O_4 was prepared as described previously [12]. Cylindrical shaped silica pellets (Aerolyst 3038, Degussa; $d_{pellet} = 2.5$ mm; $h_{pellet} = 4.5$ mm; $S_{BET} = 270$ m^2/g; $d_{pore} = 12$ nm) were contacted with an impregnation solution containing 0.55 g $Co(NO_3)_2{\cdot}6H_2O$ in 1 ml deionised water. The catalyst precursor was aged at room temperature for 20 min and dried in a ventilated oven at 120 °C for 2 h. Subsequently, the dried precursor was calcined in air (180 ml(STP)/min) at 350 °C for 2 h (heating rate: 5 °C/min). The impregnation–drying–calcination procedure was repeated twice to obtain catalyst pellets with 31.5 wt% Co_3O_4. Catalyst particles with different sizes were obtained by crushing the uniform catalyst pellet to the desired size range.

The Co_3O_4 loading of the catalytic materials was verified using AAS-ICP after acid digestion of the sample in a 4:1 HCl/HF-mixture. The distribution of the Co_3O_4 crystallites on the silica-supported catalysts was viewed using a LEO transmission electron microscope (TEM) 912 with an acceleration voltage of 120 kV. The morphology of the unsupported Co_3O_4 was viewed using a scanning electron microscope (Nova NanoSEM 230) equipped with a Four Quadrant Back Scatter detector and an energy dispersive Fissons Kevex X-ray spectrometer (EDXA) operating at 10 keV. The average crystallite size of the silica-supported Co_3O_4-catalyst was determined using X-ray diffraction (Bruker D8 advanced XRD, source Co-$K_{\alpha,1}$, voltage: 35 kV, current: 40 mA) using Rietveld refinement. The BET-surface area and micro-pore volume was determined using N_2-adsorption/desorption at 77 K using a Micromeritics Tristar 3000.

The catalytic activity of the catalysts in the ammonia oxidation was determined in a quartz, fixed bed reactor ($d_{inner} = 9$ mm, $d_{outer} = 12$ mm, $l = 410$ mm) with an isothermal zone of 20 mm (a temperature variation of less than 5 °C was obtained in the isothermal zone, which implies a variation in the rate of reaction of <4 % based on the reported activation energy of 9 kcal/mol [2]). The catalyst (either in pellet form or in powder form) was diluted with ca. 300 mg silica with a particle size of less than 75 μm (obtained by crushing Aerolyst 3038) and loaded into the isothermal zone. The high degree of dilution ($m_{diluent}/m_{catalyst} = 300$) applied in the case of the catalyst powders may result in an inhomogeneous distribution of the catalyst and bypassing of the reactants [13], however the use of fines as diluent mitigates this effect, due to extensive radial mixing. Furthermore, it was observed that repeatability of the experiments was good and deviations in terms of ammonia conversion on repeat runs were less than 2 %. The catalyst bed was supported by a bed of silicon carbide ($d_p = 425$–600 μm). A quartz thermowell ($d_{outer} = 4$ mm) was inserted into the catalyst bed to monitor the reaction temperature. A silicon carbide ($d_p = 425$–600 μm) bed ($l = 125$ mm) on top of the catalyst bed served as a pre-heating zone.

A pre-mixed gas containing 7.1 % NH_3, 19.4 % O_2 and the balance He was led over the catalyst bed at a volumetric flow rate of 100–200 ml (NTP)/min. The ammonia oxidation was performed at atmospheric pressure in the temperature range 450–600 °C. The reactor temperature was raised to the required temperature and after 30 min the ammonia conversion was determined by bubbling the effluent gas for 20–30 min through deionised water ensuring complete absorption of ammonia. The concentration of ammonia in the ammonia trap was determined spectro-photometrically using the Nessler method [14] using a Jenway 6405 UV/Vis spectrometer at 450 nm.

The selectivity of the ammonia oxidation was confirmed by loading the catalyst diluted with ca. 300 mg SiO_2 ($d_p < 75$ μm obtained by crushing Aerolyst 3038) into a U-tube quartz reactor in the Micromeritics Autochem 2910. The ammonia oxidation was performed using a pre-mixed gas containing 7.1 % NH_3, 19.4 %O_2 and the balance He, which was led over the catalyst bed at a volumetric flow rate of 100 ml (NTP)/min. The catalyst bed was heated up to 800 °C using a linear temperature ramp of 10 °C/min. The composition of the effluent was monitored with an on-line mass spectrometer (Pfeiffer Vacuum Quadrupole Mass Spectrometer 2000).

3 Results and Discussion

Table 1 gives the physical characteristics of the unsupported and supported Co_3O_4-catalysts for the ammonia

Table 1 Characterization of the fresh catalyst used

	Unsupported Co_3O_4	Supported Co_3O_4
Support	–	Silica—Aerolyst 3038
S_{BET}, m^2/g	–	270
V_{pore}, cm^3/g	–	0.92
d_{pore}, nm	–	12
Catalyst		
Co-loading, wt%	76.7	23.1
d_{pellet}, cm	0.3	0.25
h_{pellet}, cm	0.3	0.45
ρ_{pellet}, cm^3/g	3.54	0.90
Porosity, ε	0.42	0.67
V_{pore}, cm^3/g	0.12	0.75
$V_{micro\text{-}pore}$, cm^3/g	6×10^{-4}	0.63
S_{BET}, m^2/g	0.36	150
d_{pore}	1.3 μm	17 nm
dCo_3O_4	0.25–5 μm[a]	25.2 nm[b]
		24.4 ± 4.5 nm[c]

[a] Size determined using SEM

[b] Average crystallite size of Co_3O_4 crystallites using XRD

[c] Distribution of sizes of Co_3O_4 crystallites as estimated using TEM based on counting ca. 100 crystallites (with indication of the variance in the distribution)

oxidation. The cobalt loading in the unsupported Co_3O_4 was determined to be 76.7 wt%, which corresponds to pure Co_3O_4, whereas the silica-supported catalyst contains 23.1 wt% cobalt which would correspond to a Co_3O_4 loading of 31.5 wt% if all cobalt is present as Co_3O_4.

The unsupported cobalt oxide catalyst, a commercial ammonia oxidation catalyst, comprises of a wide range of irregular shaped Co_3O_4 crystallites in close proximity. The silica-supported Co_3O_4 catalysts also comprises of agglomerates of Co_3O_4 crystallites with a rather narrow size distribution (see Fig. 1; Table 1). The presence of agglomerates of Co_3O_4 crystallites on the silica-supported catalyst is inherent to the synthesis procedure starting from cobalt nitrate. The synthesis procedure leads to the formation of cobalt nitrate droplets [15], which upon calcination break up to form Co_3O_4 crystallites.

The average crystallite size of Co_3O_4 on the silica-supported catalyst was determined to be 25.2 nm (as determined by XRD), with a Co_3O_4-content in the catalyst of 23 wt% implying a relative large amount of XRD-amorphous cobalt present in the catalyst. Hence, the surface area of the Co_3O_4 crystallites in the silica-supported catalyst per unit mass of catalyst is estimated to be 8.9 $m^2/g_{catalyst}$. The intrinsic activity of the silica-supported Co_3O_4-catalyst is thus expected to be ca. 25 times larger than that of the unsupported Co_3O_4 catalyst, if the whole surface area attributable to Co_3O_4 is accessible to the reagents, and if the surface area does not change under the reaction conditions (it should be noted that a similar intrinsic surface area can have been achieved by utilising an unsupported Co_3O_4-catalyst with an average crystallite size of ca. 40 nm).

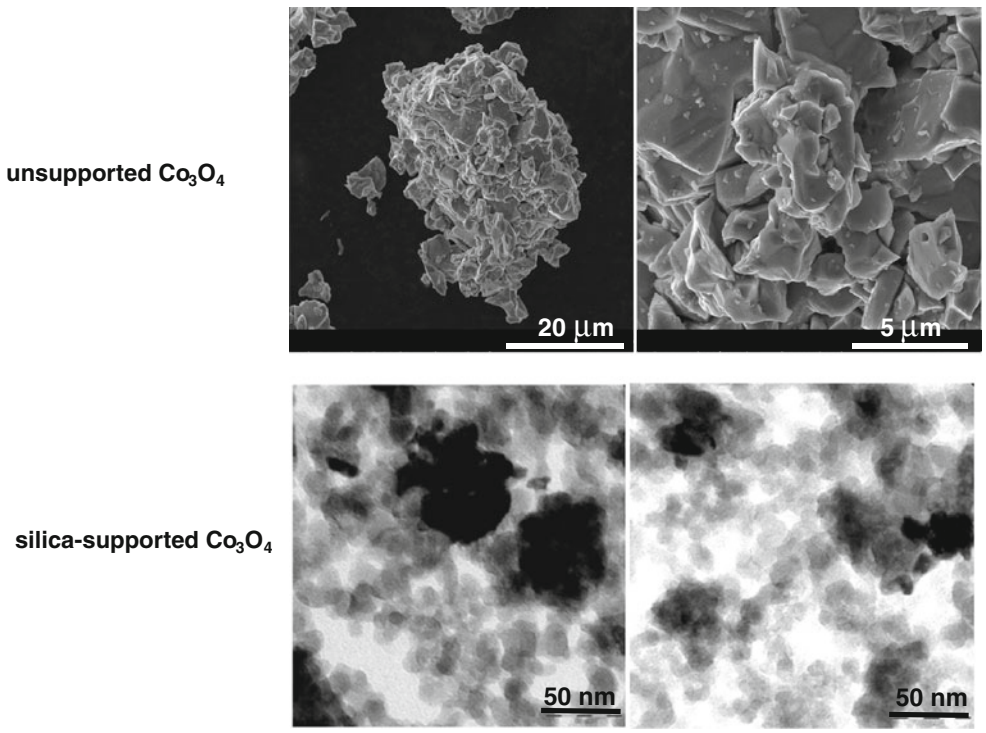

Fig. 1 SEM-images for the unsupported Co_3O_4-catalyst (*top*) and TEM-images for the silica supported Co_3O_4-catalyst (*bottom*)

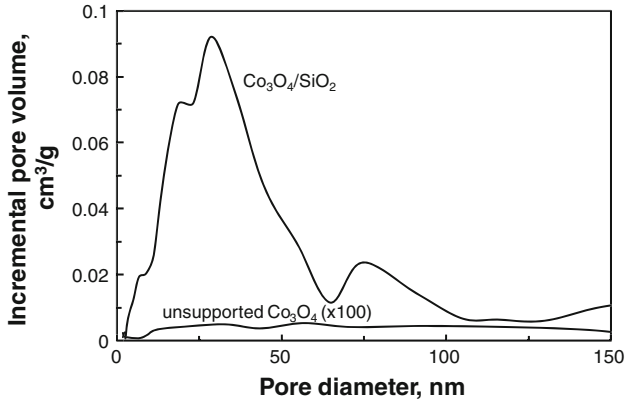

Fig. 2 Pore size distribution obtained from BJH-adsorption branch for the unsupported Co_3O_4 and Co_3O_4/SiO_2 (Note: the incremental pore volume for the unsupported Co_3O_4 is multiplied with 100)

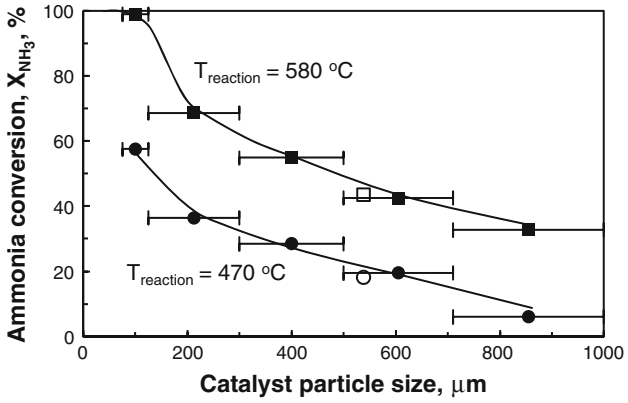

Fig. 3 Ammonia conversion at 470 °C and 580 °C over unsupported Co_3O_4 particles (*open symbols*; SV = 3.73 mmol NH_3/g/s) and silica-supported Co_3O_4 particles (*closed symbols*; SV = 4.84 mmol $NH_3/g_{catalyst}$/s) as a function of the average particle size

The unsupported Co_3O_4 catalyst contains mainly macropores, whereas the silica-supported Co_3O_4 catalyst contains mainly micro-pores (see Fig. 2). Hence, the diffusional resistance in the silica-supported catalyst is expected to be much more severe in comparison to the unsupported catalyst, since diffusion in the pores of the silica-supported catalyst is governed by Knudsen diffusion, whereas in the unsupported catalyst bulk gas diffusion contributes significantly. The effect of the reduced diffusion coefficient in the silica-supported catalyst is negated by the higher porosity in this catalyst and the lower amount of catalytically active material per unit volume of catalyst.

The ammonia oxidation in the fixed bed reactor was performed in the absence of external mass transfer limitations since doubling the linear velocity keeping the space velocity constant did not yield significant change in the conversion (see Table 2). This observation was independent of the particle size of the catalyst investigated. This observation also implies the absence of external heat transfer limitations.

Figure 3 shows the ammonia conversion as a function of the average particle size of the silica supported Co_3O_4-catalyst. The increase in the conversion level with decreasing average particle size implies severe internal mass transfer limitations. The conversion levels obtained with the crushed unsupported Co_3O_4 catalyst is slightly lower than the obtained ammonia conversion over the silica-supported Co_3O_4, despite the 25 % reduction in the space velocity and the higher loading with Co_3O_4, illustrating the effectiveness of the silica-supported catalyst. At these conversion levels the NO and N_2O are the only detected nitrogen-containing products. No N_2 was detected above the background level implying a yield of N_2 of less than 3 %. The selectivity for NO_2 (m/e = 44.4) is negligible. The NO content in the fraction of detected nitrogen containing products ($NO + N_2O$) at 540 °C is larger than 90 N%, which increases with increasing reaction temperature.

Table 2 Effect of the linear velocity on the ammonia conversion over the silica support catalyst at a space velocity of 4.84 mmol $NH_3/g_{catalyst}$/s as a function of reaction temperature

u (cm(NTP)/min)	$T_{reaction}$, °C	$d_{particle}$ = 75–125 μm (%)	$d_{particle}$ = 710–1,000 μm (%)
50	480	57.5	6.1
100	480	54.4	5.9
50	580	98.8	32. 8
100	580	96.7	29.1

The reactor performance was modelled using the rate expression reported in Sadykov et al. [2] as the intrinsic rate:

$$-r_{NH_3} = K \cdot [NH_3]^{0.36} \cdot [O_2]^{0.14} \quad (1)$$

in a plug flow model (although the flow model has little influence on the results obtained due to the low reaction orders). The intrinsic rate constant was optimised by iterative solving for the conversion assuming an isothermal catalyst bed and isothermal catalyst pellets (a maximum temperature difference between the temperature on the outside of the catalyst particle and the temperature in the centre of the catalyst particle of 3 °C was estimated). The Thiele modulus was determined based a pseudo-first order reaction:

$$\Phi = R_{particle}\sqrt{\frac{(-r_{NH_3}) \cdot \rho_{particle}}{[NH_3] \cdot D_{NH_3,eff}}} \quad (2)$$

with the effective diffusivity based on the random-pore model [16] taking into account both Knudsen diffusion and the bulk gas diffusion. The observed rate of ammonia consumption over a catalyst particle can then be estimated from:

$$\eta = \frac{3}{\Phi} \times \left(\frac{1}{\tanh(\Phi)} - \frac{1}{\Phi} \right) = \frac{-r_{NH_3,observed}}{-r_{NH_3}} \quad (3)$$

and the conversion of ammonia can be estimated by solving.

$$\frac{dX_{NH_3}}{dW} = \frac{-r_{NH_3,observed}}{F_{NH_3,inlet}} \quad (4)$$

Figure 4 shows the effectiveness factor for the unsupported and silica-supported Co_3O_4 particles as a function of the particle size. The effectiveness factor for the unsupported Co_3O_4 particles at a given average particle size is up to 20 % higher than that for the supported Co_3O_4 particles with similar average particle size. This can be attributed to a higher diffusivity of the reactants in the macro-porous system of the unsupported catalyst compared to the diffusivity in the micro-pores in the silica-supported catalyst. The effect of the higher diffusivity is however moderated by the lower porosity and the higher density of the unsupported catalyst.

For each of the particle sizes and at each temperature, the intrinsic rate constant was determined independently. The intrinsic rate constants obtained over the silica-supported

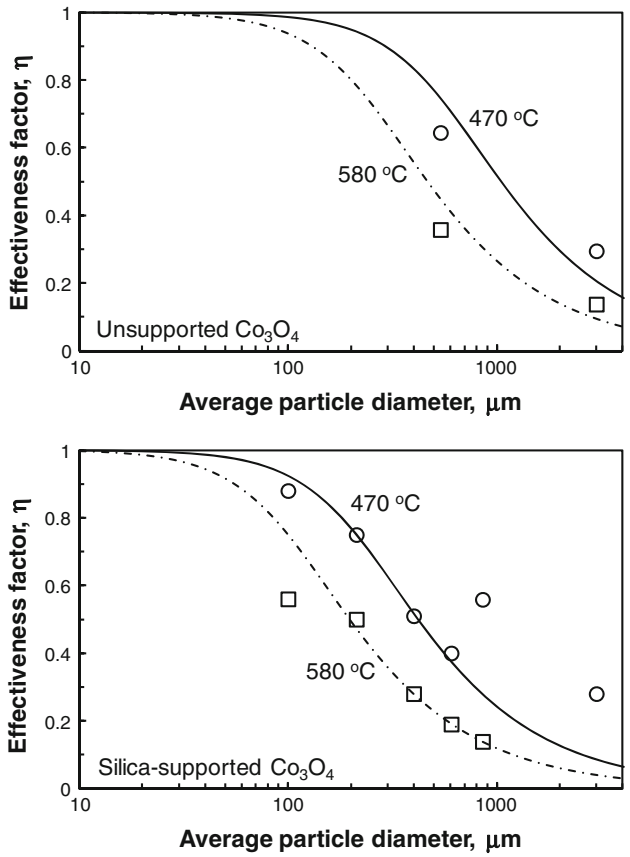

Fig. 4 Effectiveness factor of the unsupported (*top*) and silica-supported Co_3O_4 particles (*bottom*) in the oxidation of ammonia conversion at 470 and 580 °C

catalysts were consistent, i.e. $(2.1 \pm 0.5) \times 10^{-3}$ $mol^{0.5}$ $m^{1.5}/g/s$ (470 °C) and $(1.0 \pm 0.2) \times 10^{-2}$ $mol^{0.5}$ $m^{1.5}/g/s$ (580 °C) implying an activation energy of 68 ± 17 kJ/mol. The activation energy for the ammonia oxidation over the unsupported Co_3O_4 particles is in line with this and was determined to be 77 kJ/mol. The obtained activation energy is almost double the previously reported activation energy of ca. 9 kcal/mol (as reported in [2]), which may indicate that the previous measurements were determined under severe mass transfer limitations.

The determined, intrinsic rate constant for the silica-supported catalyst is on average only 3.2 times larger than that of the unsupported catalyst rather than the estimated 25 times based on the estimated oxide surface area (vide supra). The much lower than expected intrinsic rate constant for the silica-supported catalyst may be due to catalyst deactivation. A post-mortem was performed on the silica-supported catalyst pellet was characterized after being exposed to ammonia oxidation at 800 °C. The catalyst pellet contained Co_3O_4 crystallites with an average size of 26 nm according XRD, showing that sintering is negligible in the silica-supported catalyst. However Co_3O_4-content dropped significantly to ca. 11.5 wt%. Furthermore, the catalyst pellet contained Co_2SiO_4 (5 wt%) and a very small amount (ca. 0.2 wt%) of CoO. The deactivation may be caused by the partial reduction of Co_3O_4 to CoO, which upon the severe hydrothermal conditions prevalent in the reactor at high conversion levels may react to form cobalt silicate. A large amount of cobalt is unaccounted for in the spent silica-supported catalyst, which may be present in X-ray amorphous silicates. Ca. 50 % of the cobalt is unaccounted for in the spent catalyst, whereas 27 % of the cobalt is unaccounted for in the fresh catalyst indicating further transformation of cobalt into an X-ray amorphous form of cobalt. The amorphous cobalt may (partially) cover the catalytically active surface resulting in a reduced catalytic activity.

Despite the lower than expected intrinsic activity of the silica-supported catalyst and the lower effective diffusivity in the system, the effective utilisation of the catalytically active cobalt is higher with the silica-supported Co_3O_4 in comparison to the utilisation of cobalt in the unsupported Co_3O_4 (as already evidenced by the need to reduce the space velocity over the unsupported Co_3O_4 by 25 % to attain similar conversion levels as with the silica-supported catalyst—see Fig. 3). A measure for the effective utilisation of the catalytically active material would be the product of the intrinsic rate constant per unit mass of cobalt in the catalyst and the effectiveness factor. The effective utilisation of cobalt can be normalised by the activity per unit mass of cobalt in $Co_3O_4(111)$ surface (5.4 Co-atoms per nm^2 [17]). This measure of relative cobalt utilisation combines the effect of dispersion of the catalytically active

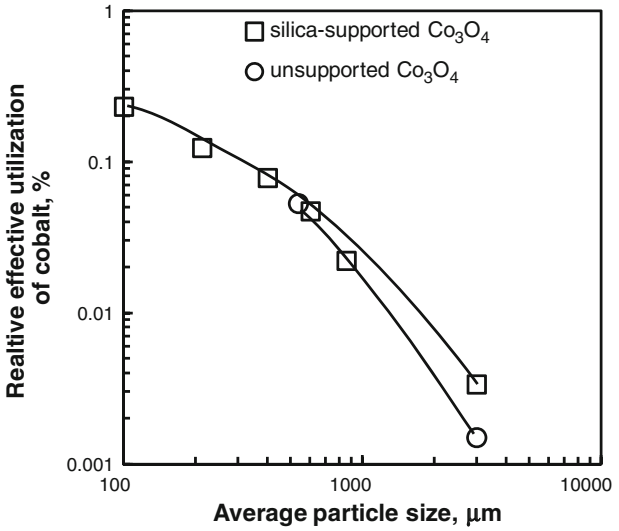

Fig. 5 Relative effective utilization of cobalt (defined as the product of the intrinsic rate constant per unit mass of cobalt and the effectiveness factor normalized by the activity per unit surface area of the crushed unsupported cobalt catalyst and a cobalt surface density of 0.52 mg/m^2) in the oxidation of ammonia conversion at 470 °C as a function of the average particle size

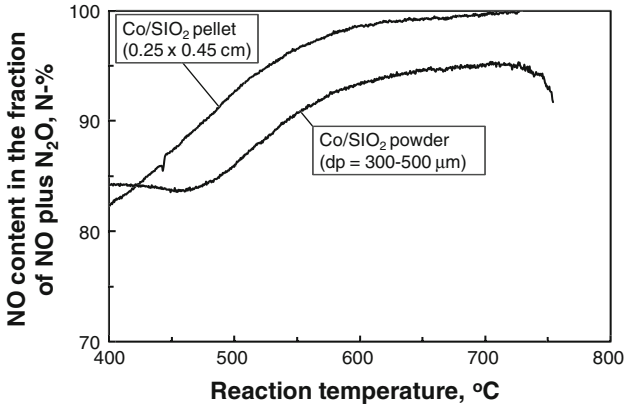

Fig. 6 NO-content in the fraction of NO + NO_2 as a function of the reaction temperature over the Co_3O_4/SiO_2-pellets (SV = 0.48 mmol NH_3/g/s) and Co_3O_4/SiO_2-powder (d_p = 300–500 µm; SV = 4.83 mmol NH_3/g/s). Reaction performed in a temperature programmed manner (heating rate: 10 C/min) using a pre-mixed gas containing 7.1 mol% NH_3, 19.4 mol% O_2 and the balance He

phase, the utilisation of cobalt to generate the catalytically active phase, catalyst deactivation (through the experimentally determined intrinsic rate constant), and mass transport limitations. Figure 5 shows the relative cobalt utilisation in the unsupported and silica-supported cobalt catalyst as a function of the average particle size taking the intrinsic rate constant obtained with the crushed unsupported Co_3O_4 as the basis for comparison and assuming that the reaction did not alter the surface area. The relative effective utilisation of cobalt in these catalysts is low mainly due to the low dispersion of Co_3O_4 in these catalysts (only 2 % of the cobalt atoms are at the surface in Co_3O_4 crystallites with an average size of 25.2 nm), showing clearly an opportunity for improving the performance of these materials as catalysts for the ammonia oxidation. The effective utilisation of cobalt as the key component in the catalytically active phase in the silica-supported cobalt catalyst is 40–120 % larger than that in the unsupported catalyst. This might be further enhanced by reducing the amount of amorphous cobalt within the catalyst.

The influence of mass transfer limitations on the selectivity of the NH_3-oxidation was investigated by flowing a pre-mixed gas containing 7.1 % NH_3, 19.4 % O_2 and the balance He was led over the supported Co_3O_4/SiO_2-catalyst in a temperature programmed manner with a linear heating rate of 10 °C/min. NO and N_2O are thought to be the primary products of the ammonia oxidation over cobalt oxide containing catalysts, which can subsequently be converted into N_2 [9]. Figure 6 shows the NO-content in the fraction of NO + NO_2 as a function of the reaction temperature of Co_3O_4/SiO_2-pellets and for Co_3O_4/SiO_2 powder with a particle diameter between 300 and 500 µm. The space velocity over the pellets was ten times less than the space velocity of the powder to account for the difference in the effectiveness factor (i.e. to obtain comparable levels of ammonia conversion). The NO content increases with increasing temperature [9] implying that the activation energy for the formation of N_2O is lower than the activation energy for the formation of NO. Furthermore, the NO-content in the fraction of NO + NO_2 is higher for the catalyst pellet. The average concentration of ammonia in the catalyst pellet is lower than the average concentration of ammonia in the 300–500 µm catalyst particles, thus resulting in a lower effectiveness factor for the ammonia oxidation (see Fig. 3). Thus, it can be concluded that the reaction order for the formation of N_2O with respect to ammonia is higher than the reaction order for the formation of NO, which is in line with the proposed reaction pathways for the formation of NO and N_2O [9]. Hence, the NO content in the fraction of NO + N_2O increases with increasing conversion level and with increasing extent of internal mass transport limitation.

4 Conclusions

Supported cobalt catalysts are more active than unsupported Co_3O_4 for the ammonia oxidation yielding NO. The obtained effectiveness factor with the supported catalyst is only slightly lower than that of the unsupported Co_3O_4, despite the lower diffusivity in the narrow pores of supported catalysts, which is partially compensated by the higher porosity and the lower catalyst density of the

silica-supported catalyst. The presence of small Co_3O_4 crystallites in the silica-supported Co_3O_4 catalyst resulted in a higher effective utilisation of cobalt within the catalyst mainly due to the higher dispersion (smaller Co_3O_4 crystallites). The effective utilisation of cobalt in the silica-supported catalysts can be improved by decreasing the average crystallite size of Co_3O_4 in the catalyst and reducing the amount of X-ray amorphous cobalt.

Acknowledgments Financial support from Trailblazer Technologies (Pty) Ltd., THRIP (TP2009070100005) and NRF (IFR20110331 00023) is gratefully acknowledged.

References

1. Clarke SI, Mazzaro WJ (2005) Nitric acid. Kirk-Othmer Encycl Chem Technol 17:1–17. doi:10.1002/0471238961.14092018031 20118.a01.pub2
2. Sadykov V, Isupova L, Zolotarskii I, Bobrova L, Noskov A, Parmon V, Brushtein E, Telyatnikova T, Chernyshev V, Lunin V (2000) Oxide catalysts for ammonia oxidation in nitric acid production: properties and perspectives. Appl Catal A 204:59–87
3. II'chenko N (1975) Catalytic oxidation of ammonia: II Relationship between catalytic properties of substances and surface oxygen bond energy. General regularities in catalytic oxidation of ammonia and organic substances. J Catal 39:73–86
4. II'chenko N, Golodets GI (1976) Catalytic oxidation of ammonia. Russ Chem Rev 45:2168–2195
5. Schmidt-Szalowski K, Krawczyk K, Petryk J (1998) The properties of cobalt oxide catalyst for ammonia oxidation. Appl Catal A 175:147–157
6. Maxwell CR (2004) Synthetic nitrogen products: a practical guide to products and process. Kluwer Academic/Plenum Press, New York
7. Ramesh S, Manharan SS, Hedge MS, Patil KC (1995) Catalytic oxidation of ammonia to nitric-oxide over La_2MO_4 (M = Co, Ni, Cu) oxides. J Catal 157:749–751
8. Pérez-Ramírez J, Vigeland B (2005) Lanthanum ferrite membranes in ammonia oxidation: opportunities for 'pocket-sized' nitric acid plants. Catal Today 105:436–442
9. Biausque G, Schuurman Y (2010) The reaction mechanism of the high temperature ammonia oxidation to nitric oxide over $LaCoO_3$. J Catal 276:306–313
10. Sun S, Rebeilleau-Dassonneville M, Zhu X, Chu W, Yang W (2010) Ammonia oxidation in $Ba_{0.5}Sr_{0.5}Co_{0.8}Fe_{0.2}O_{3-\delta}$ membrane reactor. Catal Today 149:167–171
11. de Jong KP (1999) Synthesis of supported catalysts. Curr Opin Solid State Mater Sci 4:55–62
12. Zhuang YQ, Claeys M, van Steen E (2006) Novel synthesis route for egg-shell, egg-yolk, and egg-white type of cobalt on silica catalysts. Appl Catal A 301:138–142
13. Berger RJ, Pérez-Ramírez J, Kapteijn F, Moulijn JA (2002) Catalyst performance testing: influence of catalyst bed dilution on the conversion obtained. Chem Eng J 90:173–183
14. Vogel AI (1961) Determination of ammonia. In: Mathews CK, Van Holde EK, Adhern KG (eds) Quantitative inorganic analysis, 3rd edn. Wiley, New York, pp 783–785
15. Feller A, Claeys M, van Steen E (1999) Cobalt cluster effects in zirconium promoted Co/SiO_2 Fischer-Tropsch catalysts. J Catal 185:120–130
16. Wakao N, Smith JM (1962) Diffusion in catalyst pellets. Chem Eng Sci 17:825–834
17. Zasada F, Piskorz W, Stelmachowski P, Kotarba A, Paul J-F, Płociński T, Kurzydłowski KJ, Soika Z (2011) Periodic DFT and HR-STEM studies of surface structure and morphology of cobalt spinel nanocrystals. Retrieving 3D shapes from 2D images. J Phys Chem C 115:6423–6432